Unique Conformer Selection of Human Growth-Regulatory Lectin Galectin-1 for Ganglioside GM_1 versus Bacterial Toxins[†,‡]

Hans-Christian Siebert,*[,§] Sabine André,[§] Shan-Yun Lu,[||,⊥] Martin Frank,[#] Herbert Kaltner,[§] J. Albert van Kuik,[||] Elena Y. Korchagina,[@] Nicolai Bovin,[@] Emad Tajkhorshid,[+] Robert Kaptein,[O] Johannes F. G. Vliegenthart,[||] Claus-Wilhelm von der Lieth,[#] Jesús Jiménez-Barbero,[▽] Jürgen Kopitz,[×] and Hans-Joachim Gabius*[,§]

Institut für Physiologische Chemie, Tierärztliche Fakultät, Ludwig-Maximilians-Universität München, Veterinärstrasse 13, 80539 München, Germany, Department of Bio-Organic Chemistry, Bijvoet Center for Biomolecular Research, Utrecht University, Padualaan 8, 3584 CH Utrecht, The Netherlands, College of Life Sciences, Beijing University, Beijing 100871, China, Zentrale Spektroskopie, Deutsches Krebsforschungszentrum, Im Neuenheimer Feld 280, 69120 Heidelberg, Germany, Shemyakin Institute of Bioorganic Chemistry, Russian Academy of Sciences, ul. Miklukho-Maklaya 16/10, Moscow, Russia, Theoretical and Computational Biophysics Group, Beckman Institute, University of Illinois at Urbana-Champaign, 405 North Mathews Avenue, Urbana, Illinois 61801, Department of NMR Spectroscopy, Bijvoet Center for Biomolecular Research, Utrecht University, Padualaan 8, 3584 CH Utrecht, The Netherlands, Instituto Química Orgánica y Centro de Investigaciones Biológicas, CSIC, Juan de la Cierva 3, 28006 Madrid, Spain, and Institut für molekulare Pathologie, Klinikum der Ruprecht-Karls-Universität Heidelberg, Im Neuenheimer Feld 220, 69120 Heidelberg, Germany

Received August 19, 2003; Revised Manuscript Received October 17, 2003

ABSTRACT: Endogenous lectins induce effects on cell growth by binding to antennae of natural glycoconjugates. These complex carbohydrates often present more than one potential lectin-binding site in a single chain. Using the growth-regulatory interaction of the pentasaccharide of ganglioside GM_1 with homodimeric galectin-1 on neuroblastoma cell surfaces as a model, we present a suitable strategy for addressing this issue. The approach combines NMR spectroscopic and computational methods and does not require isotope-labeled glycans. It involves conformational analysis of the two building blocks of the GM_1 glycan, i.e., the disaccharide Galβ1−3GalNAc and the trisaccharide Neu5Acα2−3Galβ1−4Glc. Their bound-state conformations were determined by transferred nuclear Overhauser enhancement spectroscopy. Next, measurements on the lectin−pentasaccharide complex revealed differential conformer selection regarding the sialylgalactose linkage in the tri- versus pentasaccharide (Φ and Ψ value of −70° and 15° vs 70° and 15°, respectively). To proceed in the structural analysis, the characteristic experimentally detected spatial vicinity of a galactose unit and Trp68 in the galectin's binding site offered a means, exploiting saturation transfer from protein to carbohydrate protons. Indeed, we detected two signals unambiguously assigned to the terminal Gal and the GalNAc residues. Computational docking and interaction energy analyses of the entire set of ligands supported and added to experimental results. The finding that the ganglioside's carbohydrate chain is subject to differential conformer selection at the sialylgalactose linkage by galectin-1 and GM_1-binding cholera toxin (Φ and Ψ values of −172° and −26°, respectively) is relevant for toxin-directed drug design. In principle, our methodology can be applied in studies aimed at blocking galectin functionality in malignancy and beyond glycosciences.

The emerging importance of the carbohydrate part of glycoconjugates for information storage and transfer is reflected in the versatile way protein- or lipid-bound cell oligosaccharides serve as sensors for productive cross-talk at the cell surface (*1*, *2*). The application of readily available plant lectins as reagents has provided ample proof of principle for the efficiency of translating such carbohydrate-dependent binding into ensuing responses, e.g., mitogenesis (*3*). This evidence and the discovery of at least five families of endogenous lectins foster the notion that their activity is involved in fundamental biological processes (*4*). Building on remarkable progress in elucidating lectin activity profiles and structures in complexes with mono- or disaccharides (*1*, *5*), the delineation of the relevant binding partners *in situ*

[†] Financial support from the EC Training and Mobility in Research program (Grant ERBFMGECT-950032), the EC program for high-level scientific conferences, RFBR 01-03-32782 (to E.Y.K.), and the Wilhelm Sander-Stiftung (Munich, Germany) is gratefully acknowledged. S.-Y.L. carried out his work with a grant from the Netherlands Organization for Scientific Research.

[‡] Dedicated to Prof. F. Cramer in respect and thankful commemoration and Prof. J. Dabrowski on the occasion of his 75th birthday.

* To whom correspondence should be addressed. E-mail: gabius@lectins.de or hsiebert@lmu.de. Telephone: ++49 89 2180 2290. Fax: ++49 89 2180 2508.

[§] Ludwig-Maximilians-Universität München.

[||] Department of Bio-Organic Chemistry, Bijvoet Center for Biomolecular Research, Utrecht University.

[⊥] Beijing University.

[#] Deutsches Krebsforschungszentrum.

[@] Russian Academy of Sciences.

[+] University of Illinois at Urbana-Champaign.

[O] Department of NMR Spectroscopy, Bijvoet Center for Biomolecular Research, Utrecht University.

[▽] CSIC.

[×] Klinikum der Ruprecht-Karls-Universität Heidelberg.

10.1021/bi035477c CCC: $25.00
Published on Web 11/21/2003

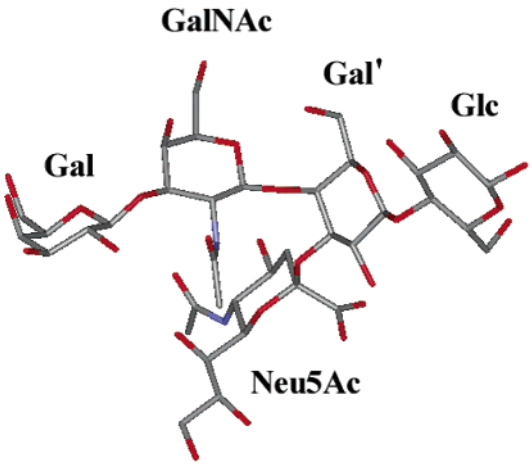

FIGURE 1: Structure of the pentasaccharide chain of ganglioside GM_1 with its two galactose moieties in central and terminal positions as potential binding sites for galectins. The Gal/Gal′ nomenclature was introduced to set these two epitopes clearly apart from each other.

and the structural details of the interaction process with these complex glycans is a major challenge. This knowledge will guide the design of synthetic mimetics with optimal positioning of the contact groups and a conformation tailored to surpass the natural ligands. Evidently, pilot studies on defined pairs of a lectin and a cell surface glycan will have to master demanding technical problems when dealing with systems of increasing complexity.

We herein address this issue by focusing on a recently found mode of interaction pivotal for growth regulation in certain tumor cells. In detail, the sialidase-dependent increase in surface presentation of ganglioside GM_1 is the control element of human neuroblastoma (SK-N-MC) cells in switching from proliferation to differentiation. A member of the lectin family of galectins, galectin-1, is the major receptor *in situ* for this saccharide-coded signal to elicit growth inhibition (*6*−*9*). The binding specificity of galectins, however, makes it clear that the elucidation of the bound-state conformation of the pentasaccharide is not the only question to be answered in this context. With the terminal Galβ1−3GalNAc epitope and the central α2,3-sialyllactose unit, the carbohydrate part of the ganglioside (see Figure 1) offers two potential binding sites (*10*−*14*). The actual contact point is, however, not known, a situation likely to be encountered frequently when dealing with complex carbohydrates of cell surfaces. We tackle these problems by a combined experimental and computational approach. First, we showed that a characteristic feature of lactose binding to galectin-1, i.e., accommodation of galactose in the vicinity of Trp68, is retained for the more complex natural ligand. Next, we ascertained ligand properties for the complete chain and two fragments by monitoring NMR[1] spectra. As far as quality of signal dispersion allowed us, we then delineated conformational aspects of the bound ligands. The experiments were flanked by molecular modeling (molecular mechanics and molecular dynamics calculations) to relate topology to energy levels. Contact sites of the ligand were inferred by picking up distinct saturation transfer from protein to certain protons. In parallel, systematic docking analysis led to elucidation of energetically favored binding modes, and the conformational scrutiny provided strong support for the conclusions based on the experimental data. Our results permit detailed comparison to the known free-state topology of the pentasaccharide (*15*, *16*) and to the way this ligand is spatially accommodated by bacterial AB_5 toxins (*17*−*19*). Because therapeutic glycomimetics blocking cell binding of the cholera toxin are being developed (*20*), our results are essential for elimination of any arising cross-reactivity between the toxins and galectins. In parallel, drug design toward galectins will also benefit from the acquired insights. Therefore, the combined approach using state-of-the-art molecular modeling and NMR spectroscopic methods will have general merit in defining contact sites and the conformation of natural lectin ligands in complex with their receptor, thereby opening the perspective for rational drug design.

MATERIALS AND METHODS

Reagents. Solvents for synthesis were routinely purified. For column chromatography, silica gel 60 (Merck, Darmstadt, Germany; particle size of 0.040−0.063 mm) was used. Thin-layer chromatography (TLC) was performed on foil plates, silica gel 60 F_{254} (Merck; catalog no. 5554, layer thickness of 0.2 mm). Sialyllactose was obtained from Sigma (Munich, Germany). Human galectin-1 was purified by affinity chromatography on lactose−Sepharose 4B, prepared after divinyl sulfone activation of the resin, as a crucial step, as described previously (*8*, *21*). Analyses of purity and quaternary structure by one- and two-dimensional gel electrophoresis and gel filtration as well as of carbohydrate binding and biological activities by solid phase assays using neoglycoprotein with GM_1-lysoganglioside as a ligand, haemagglutination, cell binding, and growth inhibition of human SK-N-MC neuroblastoma cells were performed, as described previously (*9*, *22*, *23*).

Carbohydrate Synthesis. The Thomsen−Friedenreich (TF) antigen derivative (Galβ1−3GalNAcα1-R, where R is $OCH_2CH{=}CH_2$) was synthesized as described elsewhere (*24*). The asialo-GM_1 tetrasaccharide 3-aminopropyl β-D-galactopyranosyl-(1−3)-(2-acetamido-2-deoxy-β-D-galactopyranosyl)-(1−4)-β-D-galactopyranosyl-(1−4)-β-D-glucopyranoside was prepared by block synthesis. To do this, a mixture of 3-azidopropyl *O*-(2,3,6-tri-*O*-benzyl-β-D-galactopyranosyl)-(1−4)-2,3,6-tri-*O*-benzyl-β-D-glucopyranoside (210 mg, 0.22 mmol) and molecular sieves (4 Å) in dry dichloromethane (5 mL) was stirred at room temperature under nitrogen for 30 min. The reaction mixture was cooled to −20 °C followed by addition of trimethylsilyl trifluoromethanesulfonate (0.47 μL, 2.6 μmol) in dichloromethane (47 μL) and slow dropwise addition of a solution of *O*-(2,3,4-tri-*O*-acetyl-6-*O*-benzyl-β-D-galactopyranosyl)-(1−3)-4,6-*O*-benzylidene-2-deoxy-2-(2,2,2-trichloroethoxycarbonyl)-α-D-galactopyranosyl trichloroacetimidate (250 mg, 0.26 mmol) in dry dichloromethane (5 mL). After the mixture had been stirred for 1 h at −20 °C, pyridine (10 μL) was added, and the mixture was diluted with chloroform and extracted twice

[1] Abbreviations: AMBER, assisted model building with energy refinement; CIDNP, chemically induced dynamic nuclear polarization; MD, molecular dynamics; NMR, nuclear magnetic resonance; NOESY, nuclear Overhauser and exchange spectroscopy; trNOESY, transferred NOESY; STD, saturation transfer difference; TLC, thin-layer chromatography; TOCSY, total correlation spectroscopy; TPPI, time-proportional phase incrementation.

with a 10% NaCl solution. The organic solution was dried (Na_2SO_4) and concentrated *in vacuo*. Column chromatography (toluene/ethyl acetate mixture, from 7:1 to 3:1) of the residue yielded the 3-azidopropyl *O*-(2,3,4-tri-*O*-acetyl-6-*O*-benzyl-β-D-galactopyranosyl)-(1−3)-(4,6-*O*-benzylidene-2-deoxy-2-(2,2,2-trichloroethoxycarbonyl)-β-D-galactopyranosyl)-(1−4)-(2,3,6-tri-*O*-benzyl-β-D-galactopyranosyl)-(1−4)-2,3,6-tri-*O*-benzyl-β-D-glucopyranoside (110 mg, 28%) as a colorless foam: TLC (toluene/ethyl acetate, 2:1) $R_f = 0.6$; ^{1}H NMR ($CDCl_3$) δ 1.8 (m, 2H, CH_2), 1.89, 1.97, 2.05 (3 s, 9H, Ac), 5.55 (s, 1H, CHPh), 7.1−7.53 (m, 40H, Ph). Unprotected tetrasaccharide was obtained by the following steps: removal of the benzylidene group with 80% acetic acid (70 °C, 1 h), concentration *in vacuo*, and acetylation with acetic anhydride and pyridine; reduction of the azido group with triphenyl phosphine in aqueous tetrahydrofuran followed by treatment with methyl trifluoroacetate in methanol and triethylamine; and removal of the 2,2,2-trichloroethoxycarbonyl group by zinc in acetic acid and subsequent N-acetylation by acetic anhydride, and catalytic hydrogenolysis of the benzyl ethers with palladium on charcoal followed by O-acetylation with acetic anhydride in pyridine to yield the *N*-trifluoroacetylpropyl glycoside. Column chromatography purification was performed (2:1 toluene/acetone mixture), and the tetrasaccharide was obtained in 38% yield (in four runs): TLC $R_f = 0.58$ (toluene/acetone, 1:1); ^{1}H NMR ($CDCl_3$) δ 1.9 (m, 2H, CH_2), 2.03−2.15 (m, 39H, Ac), 3.07 (m, 1H, 2c-H), 3.35, 3.52 (2m, 2H, CH_2-N), 3.58−5.42 (m, 30H); H,H-COSY δ 3.62 (5a-H), 3.75 (4a-H), 3.85 (5d-H), 4.05 (6a-H), 4.09 (4b-H), 4.44 (d, $J_{1,2} = 8$ Hz, 1b-H), 4.47 (d, $J_{1,2} = 7.7$ Hz, 1a-H), 4.58 (d, $J_{1,2} = 8$ Hz, 1d-H), 4.59 (6a-H), 4.86 (3b-H), 4.9 (2a-H), 5.0 (3c-H), 5.02 (d, $J_{1,2} = 8.2$ Hz, 1c-H), 5.1 (2d-H), 5.15 (2b-H), 5.19 (3a-H), 5.35 (4d-H), 5.39 (4c-H), 6.6 (d, $J_{2,NH} = 6.6$ Hz, 1-H, NH), 7.05 (m, 1H, $NHCOCF_3$). Finally, 2 M MeONa (10 μL) was added to a solution of this tetrasaccharide derivative (15 mg, 11 μmol) in dry methanol (0.5 mL), followed by incubation at room temperature for 6 h. Then 200 μL of water was added, before the mixture was kept overnight under the same conditions. Thereafter, it was concentrated *in vacuo*, and purification by resin H^+ column chromatography (3% aqueous NH_3) yielded the tetrasaccharide (8 mg, 98%): TLC $R_f = 0.26$ (ethanol/butanol/water/pyridine/acetic acid, 100:10:10:10:3).

Preparation of the Ganglioside GM$_1$-Released Pentasaccharide Chain. Ten milligrams of ganglioside GM_1 (Alexis, Läufelingen, Switzerland) was mixed with 3% (w/v) sodium cholate in a chloroform/methanol mixture (2:1, v/v) and dried under a stream of nitrogen. The remainder was resuspended in 10 mL of 0.1 M sodium acetate buffer (pH 5.0) and incubated at 37 °C for 48 h in the presence of 5 units of ceramide glycanase from *Macrobdella decora* (Calbiochem, Bad Soden, Germany). The reaction was stopped by the addition of 50 mL of a chloroform/methanol mixture (2:1, w/v) and vigorous mixing. After phase separation, the aqueous phase was frozen and lyophilized, the product was redissolved in 2 mL of water, for removal of ceramide, and uncleaved ganglioside was applied to prewashed C18 reversed phase SepPak cartridges (Waters, Milford, MA) and the pentasaccharide eluted with 5 mL of water (*25*). Quantification was performed by measurement of the amount of bound sialic acid (*26*). The yield was ∼90%. The purity of the compound was checked by unidirectional TLC on silica gel plates with development in two different solvent systems and detection by orcinol staining (*27*).

NMR Spectroscopic Experiments. The experiments on chemically induced dynamic nuclear polarization (CIDNP) using a continuous-wave argon ion laser (Spectra Physics, Mountain View, CA) as the source of light were performed at 33 °C with micelle-containing solutions of 2 mM GM_1 and 0.2 mM human homodimeric galectin-1. The ion laser operated in the multiline mode with emission wavelengths of 488.0 and 514.5 nm, close to the edge of the 450 nm absorption band of the added dye. The laser light was directed to the sample by an optical fiber and chopped by a mechanical shutter controlled by the spectrometer. This setup of the equipment prevented harmful heating of the protein-containing solution. As described previously, the laser photo-CIDNP radical reaction was initiated by flavin I mononucleotide (N3 of the isoalloxazine ring substituted with a CH_2COOH group and N10 with CH_3) as a laser-reactive dye, and the irradiation led to generation of protein−dye radical pairs involving dye-accessible (and therefore surface-exposed) Tyr, Trp, or His residues (*28*, *29*).

Spectra of two-dimensional (2D) NMR experiments with 2 mM ganglioside GM_1-derived pentasaccharide or its fragments in the absence or presence of 0.2 mM human galectin-1 were recorded in D_2O with Bruker AMX 500 MHz, AMX 600 MHz, and Varian Unity 750 MHz spectrometers. Assignments of the chemical shifts of the Galβ1−3GalNAc, sialyllactose, the asialo-GM_1 tetrasaccharide, and the GM_1 pentasaccharide by total correlation spectroscopy (TOCSY) were in accordance with data from literature (*30*−*33*). Nuclear Overhauser enhancement spectroscopy (NOESY and ROESY) and transferred NOESY (trNOESY) experiments were performed in the phase-sensitive mode using the time-proportional phase incrementation (TPPI) method for quadrature detection in F_1. Typically, a data matrix of 512 × 2048 points was chosen for digitization of a spectral width of 15 ppm. Eighty scans per increment were used with a relaxation delay of 1 s. Prior to Fourier transformation, zero filling was performed in the F_1 direction to expand the data set to 1024 × 2048 points. Baseline correction was applied in both dimensions. NOESY and trNOESY experiments were carried out with mixing times of 50, 100, and 200 ms to monitor buildup curves and spot spin diffusion, as described previously (*33*, *34*). The angles of the glycosidic linkage to translate the measured NOE signals from interresidual contacts into conformations are defined as follows: Φ, H1−C1−O−C′*X* (C1−C2−O−C′3 for Neu5Acα2−3Gal); and Ψ, C1−O−C′*X*−H′*X*. Saturation transfer difference (STD) (*35*−*37*) spectra were obtained by collecting 512 scans for on-resonance (Δ = 7.2 ppm) and off-resonance (Δ = 40 ppm). A total of 16 dummy scans were chosen. The internal subtraction to yield the differences was carried out by phase cycling. Selective pulses with a duration of 50 ms were used to saturate protein resonances. Measurements were taken on solutions containing 0.5 mM galectin-1 and a 10:1 molar ratio for the ligands at 33 °C.

Molecular Modeling. Docking analysis was performed with a structural model of human galectin-1, constructed through knowledge-based homology modeling using the X-ray coordinates of bovine galectin-1 (1SLT) as a template (*28*). The initial structures of the pentasaccharide and its

fragments (asialo-GM_1 tetrasaccharide, sialyllactose, or Galβ1−3GalNAc) were built using the SWEET-II Web interface (*38*; http://www.dkfz-heidelberg.de/spec/sweet2/doc/index.html) and subsequently minimized with the MM3 force field implemented in SWEET-II. Molecular dynamics (MD) simulations were performed using the AMBER force field as implemented in the DISCOVER program. The atom types and partial charges as required for the AMBER force field were assigned using the INSIGHTII software (Accelrys, San Diego, CA). Starting structures for docking and analysis of interaction energies were generated by superposition (root-mean-square deviation of <0.05 Å) of the galactose residues of the ganglioside GM_1 pentasaccharide or of its fragments on the galactose moiety of *N*-acetyllactosamine present in the crystal structure (1SLT). After the complex had been placed in a water box (50 Å × 50 Å × 50 Å), the complete molecular system was refined using 1000 steps of conjugate gradient energy minimization and 5×10^4 steps (50 ps) of equilibration with an integration time of 1 fs at 300 K. The production run included a calculation period of 1 ns with snapshots taken at 1 ps intervals. For each of the 1000 stored coordinate sets, nonbonded interactions between the protein and its ligand were computed using the stand-alone version of DISCOVER. The acquired data were further analyzed by software designed for this purpose (http://www.md-simulations.de/CAT/; for applications, see refs *37* and *39*). MD simulations were performed using DISCOVER on an IBM-SP2 parallel machine with four to eight processors.

RESULTS

GM_1 Binding to Galectin-1 Involves Interaction between Trp68 and a Galactose Residue. Our previous experiments had revealed the binding of the pentasaccharide chain of ganglioside GM_1 to galectin-1; however, they could not provide information about the relative positioning of the ligand in the lectin's receptor site. For this purpose, the laser photo-CIDNP technique establishes a sensitive tool for probing a characteristic feature of disaccharide binding to galectins, namely, the spatial vicinity of the indole ring of Trp68 and the galactose residue (*28*). In addition to galectins, the reliability of this method in detecting ligand proximity to a sensitive aromatic side chain has also been validated for hevein domain-containing plant agglutinins (*29*). The intense and sharp proton signals of Trp68, the only Trp present in the sequence, in ligand-free galectin-1 arising from the unimpaired access of dye to this site were markedly reduced in intensity in the presence of lactose (Figure 2a,b), as also shown in our previous study (*28*). Monitoring Trp signals when galectin-1 interacted with ganglioside GM_1-containing micelles produced definitive evidence for a physical interaction between the surface-presented pentasaccharide and galectin-1 (Figure 2c). Furthermore, the rather similar alterations of signals by lactose and the more complex natural ligand indicated that the relative positioning of a galactose residue in the binding site, the key factor for the extent of dye access to Trp68, was not drastically altered. The CH-π stacking between the B-face of the hexopyranose ring of galactose and the indole of Trp68, characteristic for any galectin studied so far, appeared to be preserved. Besides the prominent role of a galactose residue in this respect being proven, a valuable quality control for interpretation of results

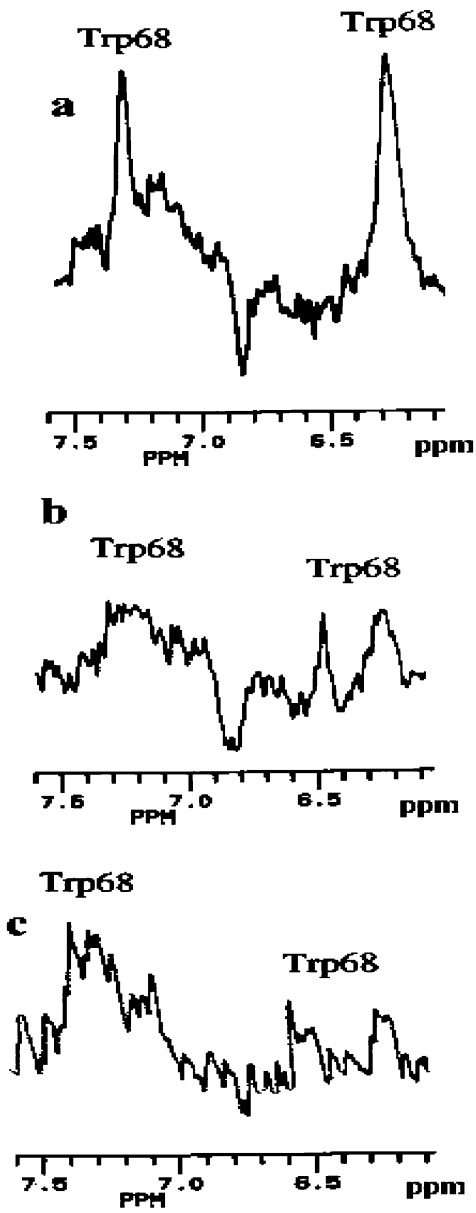

FIGURE 2: Laser photo-CIDNP difference spectra of human galectin-1 (aromatic part) in the absence of a carbohydrate ligand showing the extent of dye accessibility of the Trp68 side chain in the carbohydrate-binding site (a) and in the presence of 5 mM lactose to determine the effect of ligand binding on dye access to Trp68 (b). (c) Incubation of the lectin with ganglioside GM_1 presented in mixed micelles with dodecylphosphocholine illustrates the marked occupation of the binding site by this interaction.

from docking analysis was obtained. On the other hand, these data cannot offer a conclusive picture of which galactose unit within the ganglioside's carbohydrate chain is responsible for blocking dye access or details of the bound-state conformation of the natural ligand.

To this end, we proceeded to measure interproton distances in the carbohydrate using NOE signals as molecular rulers and to spot the occurrence of trNOE signals in the presence of galectin-1. At first, we focused on the two different galactose-containing building blocks of the pentasaccharide. Results from inhibition studies show comparatively strong potency of the trisaccharide (*10*, *12*, *13*) and nourish the hypothesis that the sialyllactose moiety of the ganglioside could act as the target site for galectin-1. The fact that the

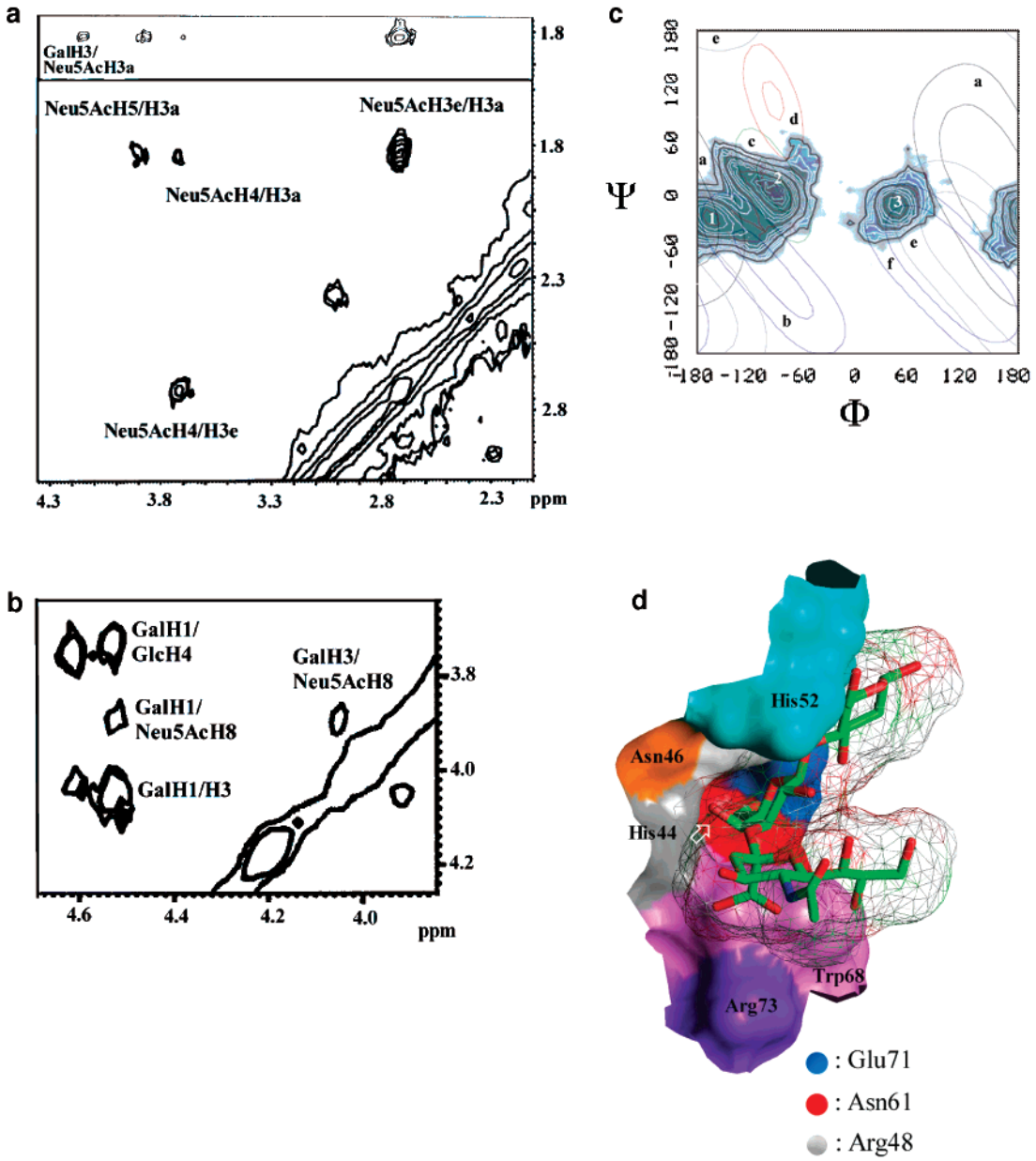

FIGURE 3: Illustration of NOE contacts between protons of the α2,3-linked *N*-acetylneuraminic acid (Neu5Ac) and galactose (Gal) moieties in sialyllactose. The disappearance of an interresidual contact visible in the 2D ROESY spectrum (a, top section) upon complexation with human galectin-1 becomes apparent in the 2D trNOE spectrum (a, bottom section), whereas the interresidual contacts between Gal H1 and Neu5Ac H8 and between Gal H3 and Neu5Ac H8 are still detectable (b). (c) The measured contact pattern in the complex favors accommodation of sialyllactose in conformation 2 from the set of the three measurable low-energy conformations present in solution as defined by their distinct combinations of Φ and Ψ (angles in the given distance map). The detectable interresidual contacts are defined as follows: (a) Neu5Ac H3a−Gal H4, (b) Neu5Ac H8−Gal H4, (c) Neu5Ac H8−Gal H3, (d) Neu5Ac H8−Gal H1, (e) Neu5Ac H3a−Gal H4, and (f) Neu5Ac H3e−Gal H4. (d) The experimental results are in perfect accord with computational docking of sialyllactose into the binding site of human galectin-1 (the white arrow marks the 4′-hydroxyl group which serves as an acceptor for chain elongation).

conformations of these ligands, when bound to a galectin, have so far not been described served as additional incentive for these experiments.

Galectin-1 Binds Both Galactose Units in Building Blocks of the Pentasaccharide Chain. At the outset, the experimental conditions were optimized by systematically studying the effects of the galectin:ligand ratio and the mixing time. In addition to evidence from line broadening and differences in chemical shifts which, for example, concern H3/H5 resonances of the sialic acid, the occurrence of characteristic cross-peaks in the trNOESY spectra clearly showed that both building blocks of the ganglioside's pentasaccharide chain harbored inherent ligand specificity. For the disaccharide, the two trNOE contacts of the Gal H1−GalNAc H3 and Gal H1−GalNAc H4 proton pairs, also visible as ROESY signals, are in agreement with the population of the global minimum conformation, calculated by molecular mechanics simulations (*33*). The two contacts are also in agreement with a maintained flexibility around the Ψ angle in the range between −30° and 15°. In contrast to retaining the interresidual signal pattern in the case of the disaccharide, the comparison of ROESY and trNOESY spectra for sialyllactose disclosed a qualitative difference, i.e., disappearance of the contact between Gal H3 and Neu5Ac H3a (Figure 3a). When present, it is consistent with two of the three low-energy conformations in solution. Combined with the

Table 1: Average Dihedral Φ and Ψ Angles of Glycosidic Linkages in the Pentasaccharide Chain of Ganglioside GM_1 Free in Solution and in Complex with Human Galectin-1 in Solution or Other Receptor Types in Crystals[a]

disaccharide/protein type[b]	Neu5Acα2−3Gal (Φ/Ψ) (deg)	Galβ1−3GalNAc (Φ/Ψ) (deg)	GalNAcβ1−4Gal (Φ/Ψ) (deg)	Galβ1−4Glc (Φ/Ψ) (deg)
ganglioside GM_1 free in solution (*15*, *16*, *52*)	−150/−10, −70/30, 80/0	50/30, 50/0, 45/−60	25/25, 0/30, −15/−30	−30/−30, 30/−15, 45/5
human galectin-1 (this study)	−	45/30, 45/0, 45/−30	−	−
human galectin-1 (this study)	−70/10	−	−	50/10, 20/−30
human galectin-1 (this study)	70/15	45/−5	25/25	−30/−30, 30/−15, 45/5
human galectin-1 (this study)	−	45/30, 45/0, 45/−30	25/25, 0/30, −15/−30	−30/−30, 30/−15, 45/5
cholera toxin (2CHB, 3CHB)	−172/−26, −174/−18	54/−9, 53/−8	44/1, 33/6	36/−27, −25/−33, −37/−13, 47/0, −34/−22, −35/−21
cholera toxin (solution) (*20*)	−	50/0	−	−
enterotoxin (*Streptomyces aureus*) (1SE3)	18/−35	−	−	−31/−35
Maackia amurensis agglutinin (1DBN)	−71/3	−	−	27/12
influenza virus hemagglutinin (1HGG)	−61/4	−	−	57/−11
wheat germ agglutinin (1WGC, 2WGC)	−63/−6, −69/6	−	−	96/−2, 67/−8
major capsid protein of the murine polyoma virus (1SID)	−53/11	−	−	72/9
sialoadhesin (1QFO)	−70/−19	−	−	37/−8
selectin-like mutant of mannan-binding lectin (1KMB)	−62/−28	−	−	−
Viscum album agglutinin (*33*)	−	45/30, 45/0, 30/−60	−	−
enterotoxin (*Escherichia coli*) (1LTI)	−	57/−10	−	−
jacalin (1M26)	−	40/−13	−	−
peanut agglutinin (2TEP)	−	42/−33	−	−
Maclura pomifera agglutinin (1JOT)	−	39/−8	−	−

[a] When available, information is also listed for building blocks of the pentasaccharide; in these cases, the dash should be read as the absence of the corresponding linkage in the respective GM_1-derived fragment. [b] The Protein Data Bank codes are given as sources for the information.

unchanged presence of the Gal H1−Neu5Ac H8 and Gal H3−Neu5Ac H8 contacts (Figure 3b), it is evident that galectin-1 selected conformation 2 for binding, as presented in the distance map with marking for the three low-energy conformations (Figure 3c). Notably, the mentioned maintained signals represent exclusive contacts for this conformation. This result was challenged by systematic computational docking of the conformational ensemble of the ligand. The snug way the individual groups of sialyllactose fit into the binding site in this conformation is presented in Figure 3d. As listed in Table 1, the accessible conformational space of the two building blocks of the ganglioside's carbohydrate part was thus differentially affected by binding. Because sialyllactose is a more potent inhibitor of the binding of galectin to asialofetuin than Galβ1−3GalNAc [an at least 20-fold difference in relative activity (*10*, *12*, *13*)], the entropic penalty by conformer selection of sialyllactose must consequently be offset by an energetically favorable set of Coulomb/van der Waals interactions. We put this assumption to the test by computational interaction analysis. Knowledge-based docking calculations confirmed the validity of the expectation (Table 2). Summing the individual terms yielded a total interaction energy of −27.7 kcal/mol for sialyllactose versus −13.0 kcal/mol for Galβ1−3GalNAc. Major portions of this difference originate from the beneficial contact with basic amino acids Arg48 and Lys63 as well as with Trp68 (please note the high degree of mobility for the disaccharide apparently having a bearing on the extent of this contact). Having first documented that (a) both galactose units in the building blocks are binding sites and (b) definite preference is given for sialyllactose, we also described the bound-state conformations of the two ligands. Extrapolation from the properties of the two parts to the complete glycan of GM_1 thus favors the trisaccharide section as the binding partner. trNOESY experiments were performed to obtain information about the bound state of the pentasaccharide.

Table 2: Comparative Interaction Analysis of the Individual Components of the Ganglioside GM_1-Derived Pentasaccharide, α2−3 Sialyllactose (SL), and the Galβ1−3GalNAc (TF) Antigen[a]

	Gal	GalNAc	Neu5Ac	Gal′	Glc	$\sum_I$	SL	TF
Arg48	−0.8	−4.3	−1.7	0.3	0.7	−5.8	−7.5	−2.4
His52	−1.9	−3.7	0.0	0.0	0.0	−5.6	−2.8	−1.7
Trp68	−2.8	0.0	−1.3	0.0	0.0	−4.1	−6.8	−4.4
Glu71	−0.9	−1.5	−0.3	0.0	0.0	−2.7	−3.8	−1.6
Asn61	−1.0	0.0	−0.2	0.0	0.0	−1.2	−1.2	−1.1
Arg111	0.0	−0.1	−1.0	0.0	0.0	−1.1	0.0	0.0
His44	−1.0	0.0	0.0	0.0	0.0	−1.0	−1.6	−1.4
Asn46	−0.9	0.0	0.0	0.0	0.0	−0.9	0.0	−0.3
Asp54	0.0	−0.5	0.0	0.0	0.0	−0.5	0.0	0.0
Val59	−0.2	0.0	0.0	0.0	0.0	−0.2	0.0	0.0
Lys63	1.0	0.1	−1.4	0.1	0.0	−0.2	−2.8	0.0
$\sum_{II}$	−8.5	−10.0	−5.9	0.4	0.7	−23.3	−26.5[b]	−12.9[c]

[a] The Coulomb/van der Waals energy terms (kilocalories per mole) of the individual interactions between the given sugar moiety [monosaccharide building blocks of GM_1 (for the pentasaccharide sequence, please see Figure 1) and its di- or trisaccharide parts] and amino acid side chains in galectin-1's binding site are listed in the order of the size of the contribution for each amino acid to the total calculated interaction energy, termed $\sum_I$. The sum of the contribution of each sugar part to the interaction energy is given as $\sum_{II}$. [b] Additional energy contribution from the interaction with Arg73 (−2.1 kcal/mol) and Asp38 (0.9 kcal/mol), yielding a total interaction energy of −27.7 kcal/mol. [c] Additional energy contribution from the interaction with Arg73 (−0.1 kcal/mol), yielding a total interaction energy of −13.0 kcal/mol.

Galectin-1 Focuses on the Terminal Galactose Unit in GM_1. For longer carbohydrate chains, the decreasing resolution of the spectra poses an inevitable problem to a clear-cut interpretation. Typically, the limited access to complex isotope-labeled ligands from mammalian cells or chemical synthesis impedes improvement of spectral dispersion. Thus, further probing by trNOESY and examination of the obtained evidence (here on the ganglioside's carbohydrate chain) are current options. Two important interresidual contacts involving the central galactose unit were clearly visible, i.e., from

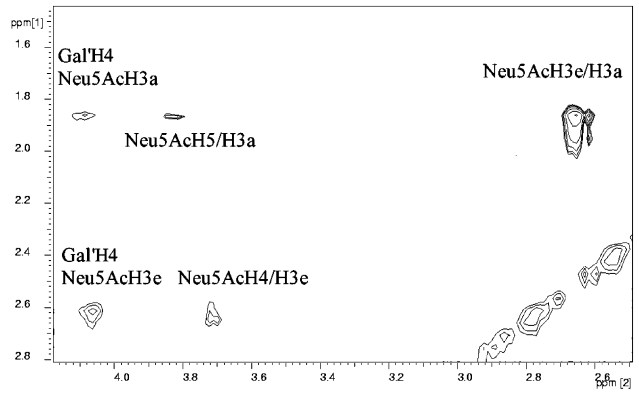

FIGURE 4: Illustration of a relevant section of the 2D trNOE spectrum of the ganglioside's pentasaccharide chain in complex with galectin-1 showing contacts of the two protons, H3a and H3e, of the sialic acid moiety with the H4 proton of the central galactose (Gal′) residue (for the complete chain structure and nomenclature, please see Figure 1).

H4 of Gal′ to H3a and H3e of Neu5Ac (Figure 4). These contacts indicated a limited flexibility around the glycosidic bond to the sialic acid moiety and a structural change relative to galectin-bound sialyllactose. On the basis of these data, the conformation of the Neu5Acα2−3Gal′ linkage apparently shifted from position 2 to position 3 in the distance map (Figure 3c). To see such a differential conformer selection happen is suggestive of a binding process at this site. Nonetheless, two points require attention. (a) This section of the conformational space of the respective glycosidic linkage is more densely populated in the pentasaccharide than in the disaccharide, and (b) ligand binding at the other galactose moiety might proceed without distortion of this distinct low-energy Φ and Ψ combination. Thus, it would be premature to interpret this result as case of conformer selection that is dependent on docking at the central galactose unit. Because of severe signal overlap, delineation of additional structural information for addressing the issue on target site selection was precluded. The trNOE spectra yet revealed no evidence of the occurrence of an *anti* conformation, as characteristic exclusive contacts remained absent. To further explore which galactose unit is in contact with Trp68, as proven by the laser photo-CIDNP experiments (Figure 2), the spatial proximity between Trp68 and galactose in the binding site might be exploited in STD experiments.

Following irradiation in the aromatic region, the hereby initiated saturation transfer to ligand protons can cause the emergence of new ligand-derived signals in the difference spectra. They will reflect the intermolecular proximity in the complex. Indeed, protons of the pentasaccharide were reactive (Figure 5, top and middle panels as well as the inset of the top panel). The illustrated control of the appearance of the STD spectrum in the absence of the ligand excludes a notable contribution of exclusively protein protons (Figure 5, inset of the top panel). Detailed comparison of the signal pattern let no evidence of significant alteration of chemical shift positions of these carbohydrate protons emerge. Line broadening is apparent. The assignment of the ligand signals, drawing on published data (*30*−*33*) and our own data (TOCSY and NOESY), revealed that the sole sources of two signals (C and D) are protons from the terminal saccharide units, whereas their involvement in the two other signals (A and B) is only likely but not proven (see the legend of Figure 5 for details). An exclusive saturation transfer to a proton of the central galactose unit was not recorded. As the presence of terminal galactose in poly-*N*-acetyllactosamine was neither sufficient nor necessary for galectin binding (*11*), we reasoned that either the sialic acid branching or the β1−4 linkage at the central galactose might be detrimental. Therefore, we synthesized a linear tetrasaccharide without the sialic acid and repeated the experiments under the same conditions. The spectrum of this sugar part continued to present signals from the terminal Gal and the GalNAc unit. The presence of further signals (E and F) assigned to these units (terminal Gal and GalNAc) further strengthened the evidence that they serve as a contact site (Figure 5). Moreover, their additional detection indicated a slight change of the relative positioning of these residues in the binding site. Up to this stage of analysis of the complex, (a) the presence of conformation 3 of the glycosidic linkage of sialylgalactose, (b) the spatial proximity of protein−ligand protons involving the two terminal sugar moieties, and (c) their selection as acceptors in saturation transfer irrespective of sialylation could be experimentally delineated. These results imply that the Galβ1−3GalNAc disaccharide, rather weakly inhibitory in inhibition assays (please see above), fittingly producing a comparatively low interaction energy (when docked as a disaccharide only; see Table 2), constituted the target site. In this respect, in-depth computational analysis was a means of accounting for the reported experimental observations.

Computational Analysis of the Complex. Computer simulations were performed to examine the entire set of models of this type of galectin−oligosaccharide interaction and to calculate interaction energies for any promising candidates. Fitting the experimental results, docking of the terminal galactose moiety into the binding site, in the measured proximity to Trp68, was readily feasible (Figure 6a). In this topology, the flexibility of the glycosidic linkage to the adjacent GalNAc moiety became restricted. The detailed profiles of the MD simulations are presented in Figure 6b, and the resulting Φ and Ψ combinations are given in Table 2. The reduced flexibility is a favorable condition for the measured saturation transfer, which could comprise contributions by His44 and -52 besides Trp68 (Figure 6a). Limiting the fluctuations in Φ and Ψ should also promote the extent of enthalpic gain. In fact, analysis of the data indicated that the GalNAc residue contributed to the interaction energy in an even stronger manner than the terminal Gal residue (−10.0 vs −8.5 kcal/mol, respectively; see Table 2). Additionally, the Neu5Ac moiety, presented on the scaffold in an energetically favorable conformation (conformer 3), contributed −5.9 kcal/mol to the overall interaction energy (Table 2). This pattern of interaction furnished an explanation for the preference for the terminal galactose unit in the complex ligand relative to the situation when testing fragments. Equally notably, attempts to dock the central galactose moiety into the vicinity of Trp68 and to accommodate the carbohydrate chain in the lectin's surface contours were invariably unsuccessful. An illustration for the problematic situation is given when looking at the neighborhood of the hydroxyl group labeled with an arrow (Figure 3d). The, at the first sight minor, difference in the occupancy of the 4′-

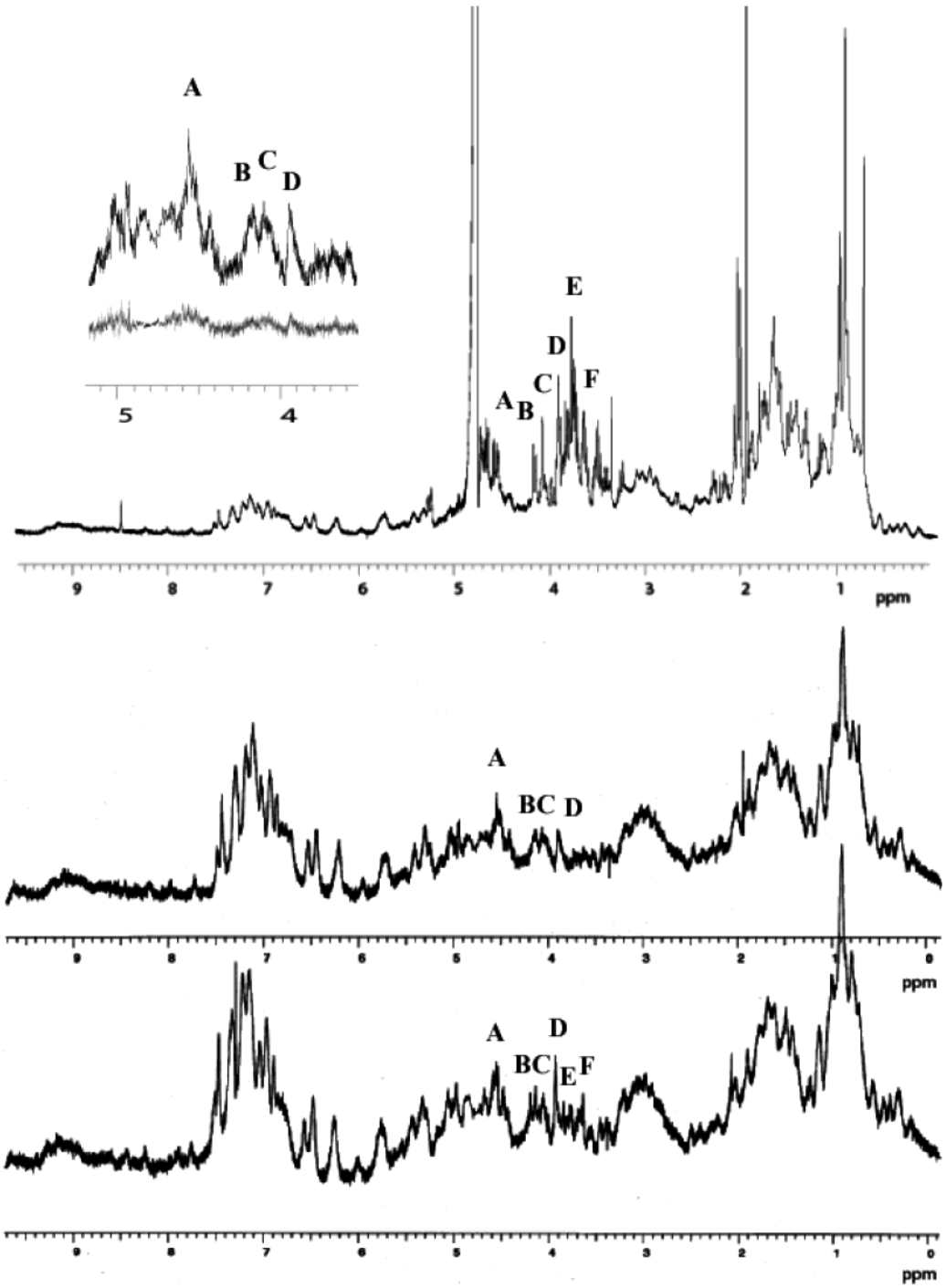

FIGURE 5: Illustration of results from STD analysis of the ganglioside's pentasaccharide chain in the presence of human galectin-1. The one-dimensional spectrum without prior saturation (top panel) is presented together with the corresponding STD spectrum (middle panel). The impact of irradiation in the aromatic region of the spectrum on proton signals of carbohydrate residues is shown [inset of the top panel: relevant section of the STD spectrum at enhanced magnification, in the presence (top) and absence (bottom) of the carbohydrate ligand with signal assignment]. The STD spectrum of the synthetic tetrasaccharide chain characteristic of the glycolipid asialo-GM_1 in complex with human galectin-1 recorded under the same saturation conditions that are used for the pentasaccharide presents two further signals, i.e., E and F (bottom panel). The following abbreviations for the signal set are given in the panels to define the carbohydrate protons involved in saturation transfer: (A) Gal H1 and/or Gal′ H1, (B) GalNAc H4 and/or Gal′ H3, (C) GalNAc H2, (D) Gal H4, (E) GalNAc H3 and GalNAc H5 (two small separate signals), and (F) Gal H3 and/or Gal H5.

hydroxyl group of the central galactose in the pentasaccharide instead of the 3′-group in chains of poly-*N*-acetyllactosamine is apparently capable of making its mark on ligand properties. The experimental and computational results thus only reach satisfying agreement with the configuration of the receptor−ligand pair shown in Figure 6a.

DISCUSSION

Ligand aggregation assays and single-molecule force microscopy revealed that galectin-1 is well suited to function as a signal inducer via its cross-linking capacity (*40*−*42*). This property can even reach the clinical level, as seen by

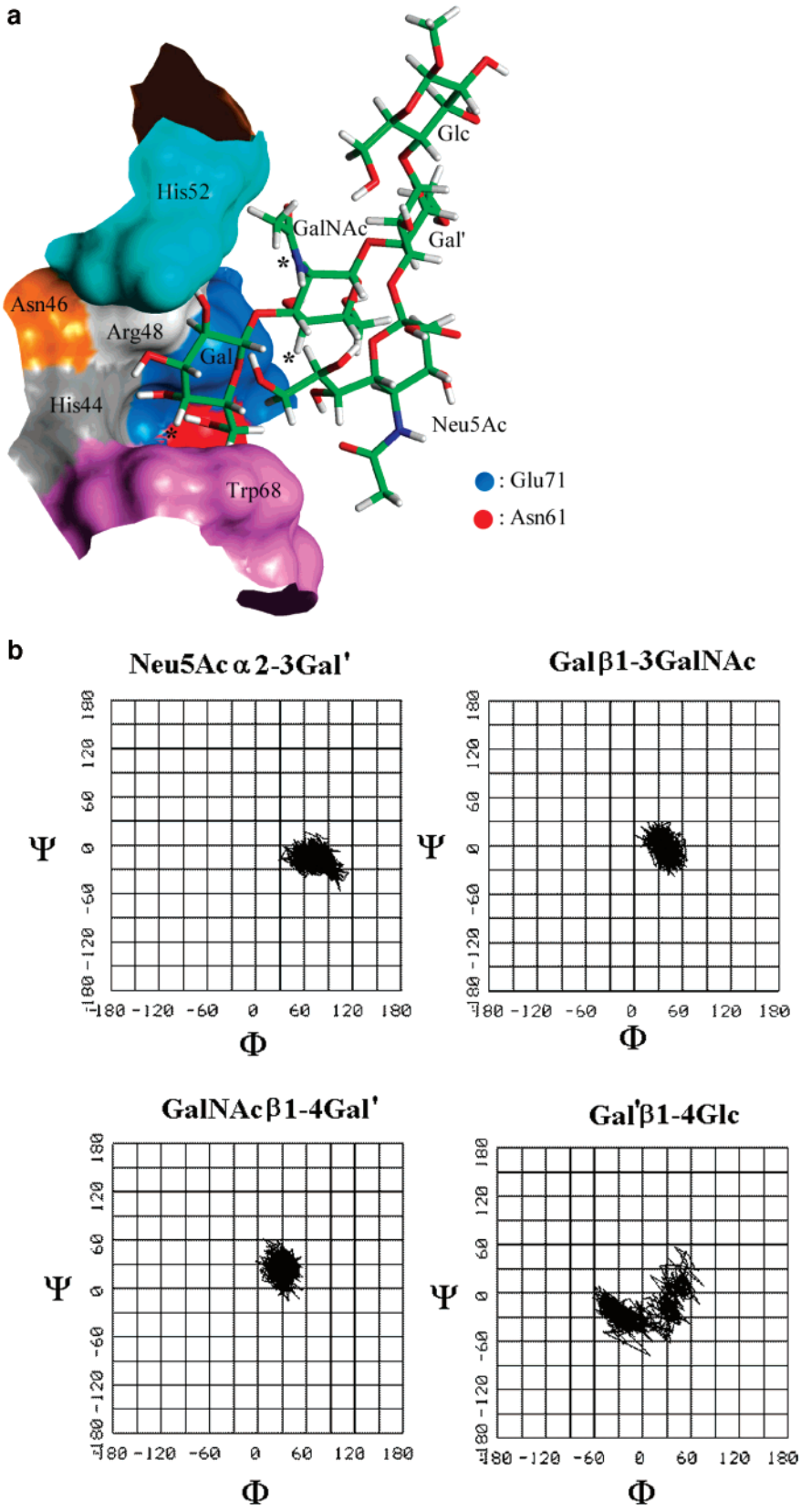

FIGURE 6: (a) Visualization of contact sites between the ganglioside's pentasaccharide and amino acid side chains in the lectin's carbohydrate-binding site (labeling with asterisks based on STD information given in Figure 5; for interaction energy terms, see Table 2 and note the contact with Trp68, as experimentally shown in Figure 2). (b) Illustration of the accessible Φ,Ψ-space based on molecular dynamics simulations for dihedral angles of each glycosidic linkage in the ganglioside's carbohydrate chain when computationally docked into the binding site of human galectin-1.

clonal selection of $CD7^-$ marker-defined classes of leukemic T cells during the progression of Sézary syndrome (*43*). In addition to glycoproteins as targets, the ability of ganglioside GM_1 to organize microdomains within a liquid-ordered phase

mimicking a raft-like structure and the prominent glycolipid headgroup presentation in rafts means it is likely to count its glycan among candidates for being a galectin target (*2*, *44*). However, solid phase assays with plastic surface-immobilized gangliosides had cast doubt on the validity of this assumption (*45*). As the mode of oligosaccharide presentation will markedly affect the interplay with a receptor, as illustrated for example for the cholera toxin (*46*), different experimental designs are required to reliably back up any conclusion. Frontal affinity chromatography with pyridylaminated ganglioside-derived oligosaccharides at pH 7.2 came up with frequent recognition (K_D values in the range of 0.5−770 μM) when GM_1, GD_{1a}, and GD_{1b} were used as ligands for six tested mammalian galectins (*47*). GM_2 failed to interact with any galectin under these conditions. In affinity electrophoresis at pH 8.3, bovine galectin-1 reacted with gangliosides in the following decreasing order of extent: from GT_{1b}, GD_{1b}, and GM_2 to GM_1 and GD_{1a} (*48*). Silica beads derivatized with lysoganglioside GM_1, a matrix for cholera toxin purification on an industrial scale, also bound human galectin-1 (*49*). In contrast to the bacterial protein, galectin-1 could be eluted from the affinity resin with 0.1 M lactose at pH 7.6 (*49*). Our previous assays for analyzing binding of galectin-1 to ganglioside-presenting microspheres, lysoganglioside-presenting neoglycoprotein, and neuroblastoma cells as well as the competition with cholera toxin in the *in vitro* experiments (*8*, *9*, *50*) corroborate the notion that, when adequately presented, the oligosaccharide chain of ganglioside GM_1 is capable of binding galectin-1. However, the lack of clear-cut physical evidence for the interaction motivated our laser photo-CIDNP experiments.

A galactose residue of the pentasaccharide blocked access of the dye to the indole ring in the binding site, a behavior which is similar to that of lactose. Literature data based on inhibition assays with the two galactose-containing building blocks, Galβ1−3GalNAc and sialyllactose (*10*, *12*, *13*), accounted for arguments for estimating which galactose residue in the glycolipid chain comes into close contact with Trp68 of the binding site. Considering the comparatively weak activity of the disaccharide (i.e., Galβ1−3GalNAc) as a competitive inhibitor, "one may suggest that the interaction occurs through an internal lactosyl of the ganglioside" (*49*), and we measured maintenance of the strong inherent flexibility of the glycosidic linkage in this disaccharide even when bound to galectin-1 (Table 2). This behavior is disparate from that of the less flexible *syn* state of bound lactose and derivatives thereof (*51*, *52*). These points arguing in favor of the central galactose unit notwithstanding, it is essential to provide direct evidence of the binding properties of the complete carbohydrate chain. By designing a strategy combining two different NMR spectroscopic techniques (trNOESY and STD monitoring) with state-of-the-art computational docking analysis, we solved this problem of target selection. We were not required to resort to the tedious preparation of isotope-labeled oligosaccharides. Notably, our approach defined in the second paragraph of the introductory section is generally relevant for addressing such an issue beyond this particular system of lectin and natural glycan.

The analysis of the way galectin-1 interacts with the carbohydrate ligands revealed several remarkable features. The trisaccharide sialyllactose and the pentasaccharide chain apparently docked to this lectin in one of the set of three low-energy conformations without any distortion of their glycosidic linkages. Our experimental evidence, especially the disappearance of the contact between Gal H3 and Neu5Ac H3 (Figure 3a), indicated selection of conformation 2 of the trisaccharide by galectin-1. A recent molecular dynamics study on bovine galectin-1 has attributed binding properties to the neighboring conformation 1 (see the energy contour map in Figure 3c) while keeping the Galβ1−4Glc torsion angles (45.1° and 14.2°) rather comparable to the experimentally and theoretically values presented in Table 1 (*53*). Thus, the two docking approaches are in accord with selection of a low-energy conformer, albeit with differences regarding the nature of the conformer. Because the origin of galectin-1 (bovine to human) differs and the shape of human galectin-1 is subject to ligand-dependent alteration in solution as determined recently by small angle neutron scattering (*54*), this effect may have a bearing on the measured preference in solution. Differences in program details in both computational protocols may also contribute to the explanation of the disparity. When one moves from the tri- to the pentasaccharide, the population density among the three low-energy conformations of sialylgalactose shown in Figure 3c will change, and this shift was reflected on the level of the bound-state conformation (Table 1 and Figure 7). Binding of galectin-1 retained the most densely populated configuration at the sialylgalactose linkage, but it no longer occurred at the sialylated galactose moiety. In fact, the target site moved to the terminal galactose residue. This result was difficult to reconcile with the mentioned inhibition data and our analysis of the interaction energy for Galβ1−3GalNAc and sialyllactose (Table 2).

When we deliberately ran docking analyses on the entire set of models without any restrictions to challenge the experimental data, exclusively this interacting mode yet appeared to be topologically feasible with adequate interaction energy terms (Figure 6a and Table 2). Evidently, a loss of the 4′-hydroxyl group contact of galactose in exchange for polar interactions with the galectin, which is seen in the crystal structure (1SLT) and the docking analysis (Figure 3d) and is inferred from chemical mapping (*55*, *56*), is a factor to be considered when engaging galactose residues in chain extensions. Thus, there is clear distinction between internal β1−3 (present in poly-*N*-acetyllactosamine chains) (*11*) and β1−4 linkages (present in gangliosides). Having hereby provided insight into why the initially assumed internal target site was neglected, we next needed to show why the terminal site could enhance its attractiveness.

An explanation was suggested by computational investigation of the complexes. Intriguingly, the rather low interaction energy of the terminal galactose unit was compensated by contributions of the GalNAc and the sialic acid moieties comfortably arrested in their well-populated low-energy conformations. As a consequence, the internal flexibility of the GalNAc moiety was reduced (Table 1 and Figure 6b), and the dihedral Φ and Ψ angles of this β1−3 linkage were locked into a position in the low-energy valley. This situation is rather common for TF-antigen-hosting lectins as well as for the cholera toxin (Table 1 and Figure 7). As part of the ganglioside's glycan, the weakly inhibitory disaccharide can thus turn into a suitable ligand for the galectin. Notably, this membrane-distal epitope is likely to be spatially accessible

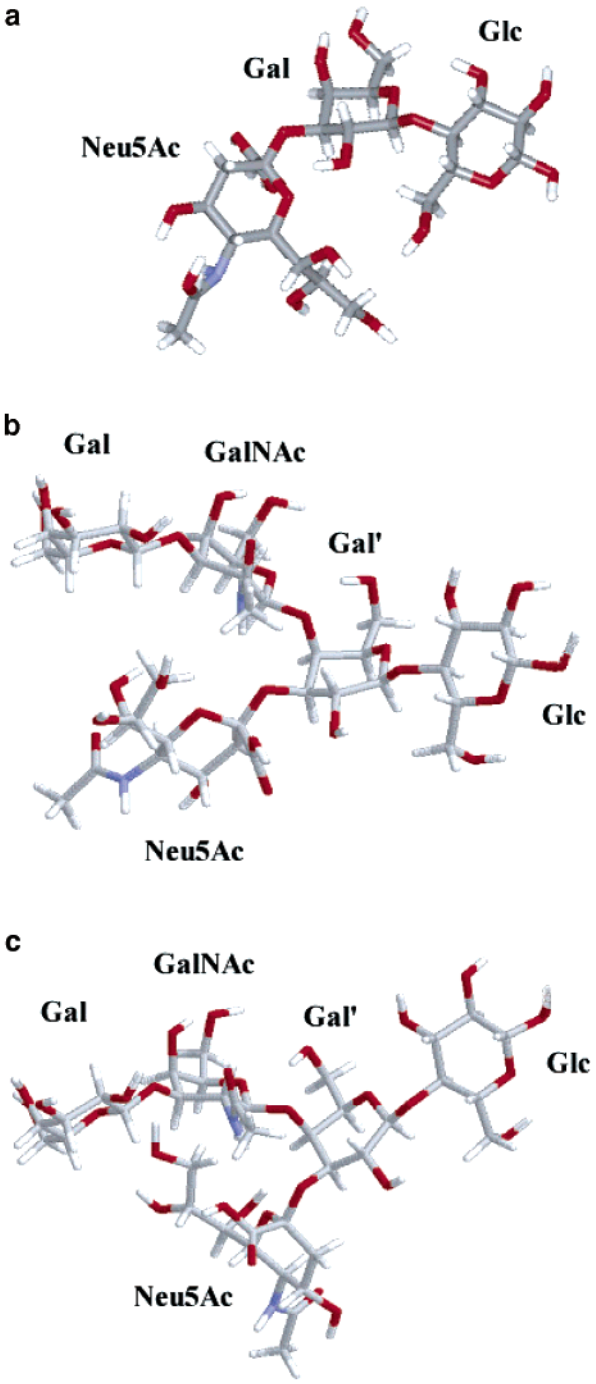

FIGURE 7: Illustration of the bound-state conformation of α2,3-linked sialyllactose in complex with human galectin-1 (a) as well as the bound-state conformations of the pentasaccharide of ganglioside GM_1 in complex with human galectin-1 (b) or cholera toxin (Protein Data Bank entry 2CHB or 3CHB, respectively) (c) showing the result of differential conformer selection.

on the cell surface for receptors. Its recognition by galectin-1 which otherwise prefers Galβ1−3(4)GlcNAc determinants teaches an instructive lesson about the versatile way the sugar code is read. Seemingly minor changes can thus translate into remarkable effects on the level of natural sugar chains. Whether the inherent ganglioside specificity of galectin-1 in our assay with magnetic beads, especially between gangliosides GM_1 and GD_{1a} (*8*), reflected structural perturbations in the glycan chain caused by new intramolecular through-space interactions (hydrogen bonding) involving the added sialic acid residue in the sugar chains of GD_{1a} (*57*) is a reasonable but not yet proven assumption. The fact that ganglioside conformation is subject to changes when its presentation is altered (*15*, *16*, *57*, *58*) is evocative of the situation when comparing different assay systems.

In view of cholera toxin's status as a drug target, it is imperative that any GM_1 mimetic will not home in on galectins. It should be emphasized that further comparison between the bound-state topologies of the pentasaccharide in the complex with either galectin-1 or cholera toxin pinpointed a clear difference, i.e., the relative positioning of the sialic acid moiety (Table 1 and Figure 7). Hydrophobic interaction with Tyr12 and hydrogen bonding to Glu11/His13 of the toxin as well as intramolecular hydrogen bonding to the two terminal units accounted for the preference for a different low-energy conformation at this site (*17*, *19*). This given documentation of differential conformer selection by galectin-1 and the bacterial toxin is relevant for the design of target-specific drugs in avoiding undesired *in vivo* cross-reactivities. Whereas valency and headgroup were factors used to discriminate between galectins and the asialoglycoprotein receptor (*59*), conformational arrest of the sialic acid moiety can be a means of excluding galectins from binding an anti-AB_5-toxin drug. Additionally, substitutions on the remaining scaffold might exploit fine-structure differences between galectins and the toxin, which harbors a patch that is suitable for hydrophobic interactions in the vicinity of the primary contact site (*60*). Equally importantly, the given strategy for delineating the binding site of a galectin in a natural glycan can direct drug design in cases where the galectin is involved in tissue invasion or metastasis, for example, galectin-1 and glioblastoma/colon cancer (*61*−*65*). This integration of the analysis of the way endogenous lectins focus on distinct sites of natural glycans into rational drug design underscores the medical perspective of the described strategy.

ACKNOWLEDGMENT

Spectrometers at the European SON NMR Large-Scale Facility in Utrecht (The Netherlands) were used in this study.

REFERENCES

1. Gabius, H.-J., André, S., Kaltner, H., and Siebert, H.-C. (2002) *Biochim. Biophys. Acta 1572*, 165−177.
2. Hakomori, S., and Handa, K. (2002) *FEBS Lett. 531*, 88−92.
3. Rüdiger, H., and Gabius, H.-J. (2001) *Glycoconjugate J. 18*, 589−613.
4. Gabius, H.-J. (1997) *Eur. J. Biochem. 243*, 543−576.
5. Solís, D., Jiménez-Barbero, J., Kaltner, H., Romero, A., Siebert, H.-C., von der Lieth, C.-W., and Gabius, H.-J. (2001) *Cells Tissues Organs 168*, 5−23.
6. Kopitz, J., von Reitzenstein, C., Mühl, C., and Cantz, M. (1994) *Biochem. Biophys. Res. Commun. 199*, 1188−1193.
7. Kopitz, J., Mühl, C., Ehemann, V., Lehmann, C., and Cantz, M. (1997) *Eur. J. Cell Biol. 73*, 1−9.
8. Kopitz, J., von Reitzenstein, C., Burchert, M., Cantz, M., and Gabius, H.-J. (1998) *J. Biol. Chem. 273*, 11205−11211.
9. Kopitz, J., von Reitzenstein, C., André, S., Kaltner, H., Uhl, J., Ehemann, V., Cantz, M., and Gabius, H.-J. (2001) *J. Biol. Chem. 276*, 35917−35923.
10. Sparrow, C. P., Leffler, H., and Barondes, S. H. (1987) *J. Biol. Chem. 262*, 7383−7390.
11. Merkle, R. A., and Cummings, R. D. (1988) *J. Biol. Chem. 263*, 16143−16149.

12. Ahmed, H., Allen, H. J., Sharma, A., and Matta, K. L. (1990) *Biochemistry 29*, 5315−5319.
13. Ahmad, N., Gabius, H.-J., Kaltner, H., André, S., Kuwabara, I., Liu, F.-T., Oscarson, S., Norberg, T., and Brewer, C. F. (2002) *Can. J. Chem. 80*, 1096−1104.
14. Wu, A. M., Wu, J. H., Tsai, M.-S., Liu, J.-H., André, S., Wasano, K., Kaltner, H., and Gabius, H.-J. (2002) *Biochem. J. 367*, 653−664.
15. Acquotti, D., Poppe, L., Dabrowski, J., von der Lieth, C.-W., Sonnino, S., and Tettamanti, G. (1990) *J. Am. Chem. Soc. 112*, 7772−7778.
16. Brocca, P., Berthault, P., and Sonnino, S. (1998) *Biophys. J. 74*, 309−318.
17. Merritt, E. A., Sarfaty, S., van den Akker, F., L'hoir, C., Martial, J. A., and Hol, W. G. J. (1994) *Protein Sci. 3*, 166−175.
18. Merritt, E. A., Sixma, T. K., Kalk, K. H., van Zanten, B. A. M., and Hol, W. G. J. (1994) *Mol. Microbiol. 13*, 745−753.
19. Merritt, E. A., Sarfaty, S., Jobling, M. G., Chang, T., Holmes, R. K., Hirst, T. R., and Hol, W. G. J. (1997) *Protein Sci. 6*, 1516−1528.
20. Bernardi, A., Potenza, D., Capelli, A. M., García-Herrero, A., Cañada, F. J., and Jiménez-Barbero, J. (2002) *Chem. Eur. J. 8*, 4598−4612.
21. Gabius, H.-J. (1990) *Anal. Biochem. 189*, 91−94.
22. Gabius, S., Kayser, K., Hellmann, K.-P., Ciesiolka, T., Trittin, A., and Gabius, H.-J. (1990) *Biochem. Biophys. Res. Commun. 169*, 239−244.
23. André, S., Pieters, R. J., Vrasidas, I., Kaltner, H., Kuwabara, I., Liu, F.-T., Liskamp, R. M. J., and Gabius, H.-J. (2001) *ChemBioChem 2*, 822−830.
24. Gabius, H.-J., Schröter, C., Gabius, S., Brinck, U., and Tietze, L.-F. (1990) *J. Histochem. Cytochem. 38*, 1625−1631.
25. Bäcker, A. E., Holgersson, J., Samuelsson, B. E., and Karlsson, H. (1998) *Glycobiology 8*, 533−545.
26. Skoza, L., and Mohos, S. (1976) *Biochem. J. 159*, 457−462.
27. Sewell, A. C. (1979) *Clin. Chim. Acta 92*, 411−414.
28. Siebert, H.-C., Adar, R., Arango, R., Burchert, M., Kaltner, H., Kayser, G., Tajkhorshid, E., von der Lieth, C.-W., Kaptein, R., Sharon, N., Vliegenthart, J. F. G., and Gabius, H.-J. (1997) *Eur. J. Biochem. 249*, 27−38.
29. Siebert, H.-C., von der Lieth, C.-W., Kaptein, R., Beintema, J. J., Dijkstra, K., van Nuland, N., Soedjanaatmadja, U. M. S., Rice, A., Vliegenthart, J. F. G., Wright, C. S., and Gabius, H.-J. (1997) *Proteins 28*, 268−284.
30. Dorland, L., van Halbeek, H., Vliegenthart, J. F. G., Schauer, R., and Wiegandt, H. (1986) *Carbohydr. Res. 151*, 233−245.
31. Ong, R. L., and Yu, R. K. (1986) *Arch. Biochem. Biophys. 245*, 157−166.
32. Siebert, H.-C., Reuter, G., Schauer, R., von der Lieth, C.-W., and Dabrowski, J. (1992) *Biochemistry 31*, 6962−6971.
33. Gilleron, M., Siebert, H.-C., Kaltner, H., von der Lieth, C.-W., Kozár, T., Halkes, K. M., Korchagina, E. Y., Bovin, N. V., Gabius, H.-J., and Vliegenthart, J. F. G. (1998) *Eur. J. Biochem. 252*, 416−427.
34. Siebert, H.-C., Gilleron, M., Kaltner, H., von der Lieth, C.-W., Kozár, T., Bovin, N. V., Korchagina, E. Y., Vliegenthart, J. F. G., and Gabius, H.-J. (1996) *Biochem. Biophys. Res. Commun. 219*, 205−212.
35. Mayer, M., and Meyer, B. (1999) *Angew. Chem., Int. Ed. 38*, 1784−1788.
36. Klein, J., Meinecke, R., Mayer, M., and Meyer, B. (1999) *J. Am. Chem. Soc. 121*, 5336−5337.
37. Siebert, H.-C., Lu, S.-Y., Frank, M., Kramer, J., Wechselberger, R., Joosten, J., André, S., Rittenhouse-Olson, K., Roy, R., von der Lieth, C.-W., Kaptein, R., Vliegenthart, J. F. G., Heck, A. J. R., and Gabius, H.-J. (2002) *Biochemistry 41*, 9707−9717.
38. Bohne, A., Lang, E., and von der Lieth, C.-W. (1998) *J. Mol. Model. 4*, 33−43.
39. Siebert, H.-C., André, S., Asensio, J. L., Cañada, F. J., Dong, X., Espinosa, J. F., Frank, M., Gilleron, M., Kaltner, H., Kozár, T., Bovin, N. V., von der Lieth, C.-W., Vliegenthart, J. F. G., Jiménez-Barbero, J., and Gabius, H.-J. (2000) *ChemBioChem 1*, 181−195.
40. Dettmann, W., Grandbois, M., André, S., Benoit, M., Wehle, A. K., Kaltner, H., Gabius, H.-J., and Gaub, H. E. (2000) *Arch. Biochem. Biophys. 383*, 157−170.
41. Brewer, C. F. (2002) *Biochim. Biophys. Acta 1572*, 255−262.
42. Gabius, H.-J. (2001) *Biochimie 83*, 659−666.
43. Rappl, G., Abken, H., Muche, J. M., Sterry, W., Tilgen, W., André, S., Kaltner, H., Ugurel, S., Gabius, H.-J., and Reinhold, U. (2002) *Leukemia 16*, 840−846.
44. Yuan, C., Furlong, J., Burgos, P., and Johnston, L. J. (2002) *Biophys. J. 82*, 2526−2535.
45. Ahmed, H., Bianchet, M. A., Amzel, L. M., Hirabayashi, J., Kasai, K.-i., Giga-Hama, Y., Tohda, H., and Vasta, G. R. (2002) *Glycobiology 12*, 451−461.
46. MacKenzie, C. R., Hirama, T., Lee, K. K., Altman, E., and Young, N. M. (1997) *J. Biol. Chem. 272*, 5533−5538.
47. Hirabayashi, J., Hashidate, T., Arata, Y., Nishi, N., Nakamura, T., Hirashima, M., Urashima, T., Oka, T., Futai, M., Müller, W. E. G., Yagi, F., and Kasai, K.-i. (2002) *Biochim. Biophys. Acta 1572*, 232−254.
48. Kannan, V. M., and Appukuttan, P. S. (1997) *Ind. J. Biochem. Biophys. 34*, 249−252.
49. Caron, M., Joubert-Caron, R., Cartier, J. R., Chadli, A., and Bladier, D. (1993) *J. Chromatogr. 646*, 327−333.
50. Kopitz, J., André, S., von Reitzenstein, C., Versluis, K., Kaltner, H., Pieters, R. J., Wasano, K., Kuwabara, I., Liu, F.-T., Cantz, M., Heck, A. J. R., and Gabius, H.-J. (2003) *Oncogene 22*, 6277−6288.
51. Asensio, J. L., Espinosa, J. F., Dietrich, H., Cañada, F. J., Schmidt, R. R., Martín-Lomas, M., André, S., Gabius, H.-J., and Jiménez-Barbero, J. (1999) *J. Am. Chem. Soc. 121*, 8995−9000.
52. Alonso-Plaza, J. M., Canales, M. A., Jiménez, M., Roldán, J. L., García-Herrero, A., Iturrino, L., Asensio, J. L., Cañada, F. J., Romero, A., Siebert, H.-C., André, S., Solís, D., Gabius, H.-J., and Jiménez-Barbero, J. (2001) *Biochim. Biophys. Acta 1568*, 225−236.
53. Ford, M. G., Weimar, T., Köhli, T., and Woods, R. J. (2003) *Proteins 53*, 229−240.
54. He, L., André, S., Siebert, H.-C., Helmholz, H., Niemeyer, B., and Gabius, H.-J. (2003) *Biophys. J. 85*, 511−524.
55. Solís, D., Jiménez-Barbero, J., Martín-Lomas, M., and Díaz-Mauriño, T. (1994) *Eur. J. Biochem. 223*, 107−114.
56. Rüdiger, H., Siebert, H.-C., Solís, D., Jiménez-Barbero, J., Romero, A., von der Lieth, C.-W., Diaz-Mauriño, T., and Gabius, H.-J. (2000) *Curr. Med. Chem. 7*, 389−416.
57. Scarsdale, J. N., Prestegard, J. H., and Yu, R. K. (1990) *Biochemistry 29*, 9843−9855.
58. Jones, D. H., Barber, K. R., and Grant, C. W. M. (1996) *Biochemistry 35*, 4803−4811.
59. André, S., Frisch, B., Kaltner, H., Desouza, D. L., Schuber, F., and Gabius, H.-J. (2000) *Pharmaceut. Res. 17*, 985−990.
60. Fan, E., Merritt, E. A., Zhang, Z., Pickens, J. C., Roach, C., Ahn, M., and Hol, W. G. J. (2001) *Acta Crystallogr. D57*, 201−212.
61. Gabius, H.-J. (1997) *Cancer Invest. 15*, 454−464.
62. Gabius, H.-J. (2001) *Anat., Histol., Embryol. 30*, 3−31.
63. Camby, I., Belot, N., Lefranc, F., Sadeghi, N., de Launoit, Y., Kaltner, H., Musette, S., Darro, F., Danguy, A., Salmon, I., Gabius, H.-J., and Kiss, R. (2002) *J. Neuropathol. Exp. Neurol. 61*, 585−596.
64. Nagy, N., Legendre, H., Engels, O., André, S., Kaltner, H., Wasano, K., Zick, Y., Pector, J.-C., Decaestecker, C., Gabius, H.-J., Salmon, I., and Kiss, R. (2003) *Cancer 97*, 1849−1858.
65. Lahm, H., André, S., Hoeflich, A., Kaltner, H., Siebert, H.-C., Sordat, B., von der Lieth, C.-W., Wolf, E., and Gabius, H.-J. (2003) *Glycoconjugate J.* (in press).

BI035477C